Supporting Information

Light-programmable, high drug-loading nanomedicine based on dimeric camptothecin

Lei Wu[a, 1], Yehan Wang [a,1], Kaimin Cai[b,1], Yang Zhou[a], Yong Wang[c], Jianjun Cheng[d,*], Hua He[a,*], Lichen Yin[a,*]

[a] Jiangsu Key Laboratory for Carbon-Based Functional Materials and Devices, Institute of Functional Nano & Soft Materials (FUNSOM), Collaborative Innovation Center of Suzhou Nano Science & Technology, Soochow University, Suzhou 215123, China.

[b] Department of Materials Science and Engineering, University of Illinois at Urbana-Champaign, Urbana, Illinois 61801, United States.

[c] Ophthalmology Department, Affiliated Nantong Clinical College of Nantong University, Nantong First People's Hospital, Nantong, Jiangsu, China

[d] School of Engineering, Westlake University, Hangzhou 310030, Zhejiang, China.

* Corresponding authors. E-mail: lcyin@suda.edu.cn (L. Yin); hhe@henau.edu.cn (H. He); chengjianjun@westlake.edu.cn (J. Cheng)

[1] Lei Wu, Yehan Wang, and Kaimin Cai contributed equally.

Supplementary methods

1. Instrumentation

NMR spectra were recorded on a Varian U500 (500 MHz) or VXR-500 (500 MHz) spectrometer. All chemical shifts were reported in part per million (ppm). HPLC analysis was performed on a 1200 Infinitely Series (Agilent Technologies, Santa Clara, CA, USA) equipped with a UV detector and an analytical C18 column (4.6 × 100 mm, 3.5 μm). Fluorescence was measured on a Perkin-Elmer LS55 fluorescence spectrometer. The particle size of NPs was determined by the Zetasizer Nano ZS90 (Malvern Instruments, Ltd., UK) and the morphology was observed by TEM (TECNAI G2, FEI, US).

2. Synthesis of hQ-NH

hQ-NHS ester (1.39 g, 4.0 mmol) and DIPEA (2.0 mL) were dissolved in dichloromethane (DCM, 20 mL), and *N*, *N'*-dimethyl-ethylene diamine (4.30 mL, 40 mmol, 10 equiv) was added. The mixture was stirred at RT for 30 min. After the solvent was removed under vacuum, the residue was redissolved in ethyl acetate (60 mL), washed with water (60 mL × 4) and saturated NaCl solution (60 mL × 3), dried over Na_2SO_4, and concentrated under vacuum, obtaining yellow powder as a mixture of mono-substituted and di-substituted amide, which was used for the next-step reaction without further purification. ESI-MS (*m*/*z*): $[M + H]^+$ calculated for $C_{18}H_{29}N_2O_3^+$, 321.2; found 321.2.

3. Synthesis of hQ-BHP-OTBS

BHP (793 mg, 2.0 mmol), triphosgene (208 mg, 0.70 mmol, 0.35 equiv), and *N*, *N*-dimethylaminopyridine (732 mg, 6.0 mmol, 3.0 equiv) were dissolved in DCM (60 mL) and stirred at RT for 15 min to afford a white suspension. A DCM solution (10 mL) of hQ-NH (640 mg, 2.0 mmol, 1.0 equiv) was then added in one portion to the suspension, during which the insoluble precipitate gradually dissolved. The mixture was then stirred at RT for 1 h and was subjected to purification by column chromatography (hexane:EtOAc, 8:1, v/v). The product was obtained as yellow powder (1.20 g, yield 81%). ^{1}H NMR (500 MHz, $CDCl_3$) δ 7.18 (s, 2H), 4.60 (s, 4H), 3.43 (m, 4H), 3.23-2.85 (m, 8H), 2.34 (s, 3H), 2.14 (s, 3H), 1.92 (m, 6H), 1.43 (s, 6H), 0.92 (s, 18H), 0.06 (s, 12H).[1] ^{13}C NMR (126 MHz, $CDCl_3$) δ 191.1, 187.5, 172.3, 154.5, 153.9, 153.6, 143.2 138.0, 136.3, 135.3, 133.3, 128.2, 60.5, 53.4, 47.8, 45.6,

[1] NMR revealed a mixture of the stereoisomer of the amide, only one set of the NMR peaks are reported here.

37.7, 36.4, 35.7, 28.7, 25.9, 21.3, 14.1, 12.6, 12.0, -5.2, -5.3. HRMS-ESI (*m/z*): $[M + H]^+$ calcd for $C_{40}H_{67}N_2O_7Si_2^+$, 743.4482; found 743.4474.

4. Synthesis of hQ-BHP-OH

hQ-BHP-OTBS (930 mg) was dissolved in a mixture of DCM/MeOH (40 mL/10 mL) and the solution was stirred with amberlyst-15 (110 mg) overnight. After completion of the reaction as monitored by TLC, the mixture was filtered, concentrated, and subjected to flash column (hexane:EtOAc, 1:2, v/v to EtOAc:MeOH, 15:1, v/v) to obtain the product as yellow solid (610 mg, yield 95%). ^{1}H NMR (500 MHz, $CDCl_3$) δ 7.19 (s, 2H), 4.50 (s, 4H), 3.75-3.40 (m, 4H), 3.25-2.96 (m, 8H), 2.80 (s, 2H), 2.33 (s, 3H), 2.11 (s, 3H), 1.96-1.78 (m, 6H), 1.41 (s, *J* = 8.0 Hz, 5H).[2] ^{13}C NMR (126 MHz, $CDCl_3$) δ 191.5, 187.6, 172.8, 156.0, 155.4, 154.5, 144.9, 143.1, 138.2, 136.4, 133.4, 129.9, 60.5, 47.7, 46.9, 44.9, 37.8, 36.3, 31.5, 28.7, 20.9, 14.2, 12.6, 11.9. HRMS-ESI (*m/z*): $[M + H]^+$ calcd for $C_{28}H_{39}N_2O_7^+$, 515.2747; found 515.2755.

5. Synthesis of Boc-OTBS$_2$

BHP (110 mg, 0.28 mmol), triphosgene (27 mg, 0.092 mmol, 0.33 equiv), and *N, N*-dimethylaminopyridine (85 mg, 0.69 mmol, 2.5 equiv) were dissolved in DCM (8 mL) and stirred at RT for 15 min to afford a white suspension. Then, a DCM solution (1 mL) of *tert*-butyl-*N*-methyl-*N*-[2-(methylamino)ethyl]carbamate (44 mg, 0.23 mmol) was added in one portion to the suspension, and the insoluble precipitate gradually dissolved. The mixture was stirred at RT for 1 h and was then subjected to purification by column chromatography (hexane:EtOAc, 10:1-8:1, v/v). The product was obtained as colorless oil (85 mg, yield 60%). ^{1}H NMR (500 MHz, $CDCl_3$), δ 7.19 (s, 2H), 4.61 (s, 4H), 3.31-3.68 (m, 4H), 2.86-3.22 (m, 6H), 2.34 (s, 3H), 1.46 (s, 9H), 0.92 (s, 18H), 0.07 (s, 12H).[3] ^{13}C NMR (126 MHz, $CDCl_3$), 154.0, 153.8, 142.9, 135.3, 133.4, 133.3, 127.1, 60.5, 60.3, 47.6, 47.4, 35.5, 35.3, 28.5, 26.0, 21.4, 18.5, -5.1. HRMS-ESI (*m/z*): $[M + H]^+$ calcd for $C_{31}H_{59}N_2O_6Si_2^+$, 611.3906; found 611.3915.

6. Synthesis of Boc-OH$_2$

[2] NMR revealed a mixture of 4 stereoisomers of the amide/urethane bonds, only one set of the NMR peaks are reported here.

[3] NMR revealed a mixture of 4 stereoisomer of the amide/urethane bonds, only one set of the NMR peaks are reported here.

Boc-OTBS$_2$ (387 mg, 0.63 mmol) was dissolved in MeOH (10 mL) and the solution was stirred with amberlyst-15 (10 mg) overnight. After the reaction was completed as monitored by TLC, the mixture was filtered, concentrated, and subjected to flash column (EtOAc to EtOAc:MeOH 10:1). The product was obtained as colorless oil (161 mg, yield 67%). ^{1}H NMR (500 MHz, $CDCl_3$), δ 7.14 (s, 2H), 4.46 (s, 4H), 2.78-3.65 (m, 14H), 2.28 (s, 3H), 1.40 (s, 9H).[4] ^{13}C NMR (126 MHz, $CDCl_3$), δ 155.8, 155.6, 136.1, 133.4, 130.4, 130.0, 80.3, 60.3, 50.4, 47.0, 35.6, 35.0, 28.5, 20.9. HRMS-ESI (*m/z*): $[M + Na]^+$ calcd for $C_{19}H_{30}N_2NaO_6^+$, 405.1991; found 405.1995.

[4] NMR revealed a mixture of 4 stereoisomer of the amide/urethane bonds, only one set of the NMR peaks are reported here.

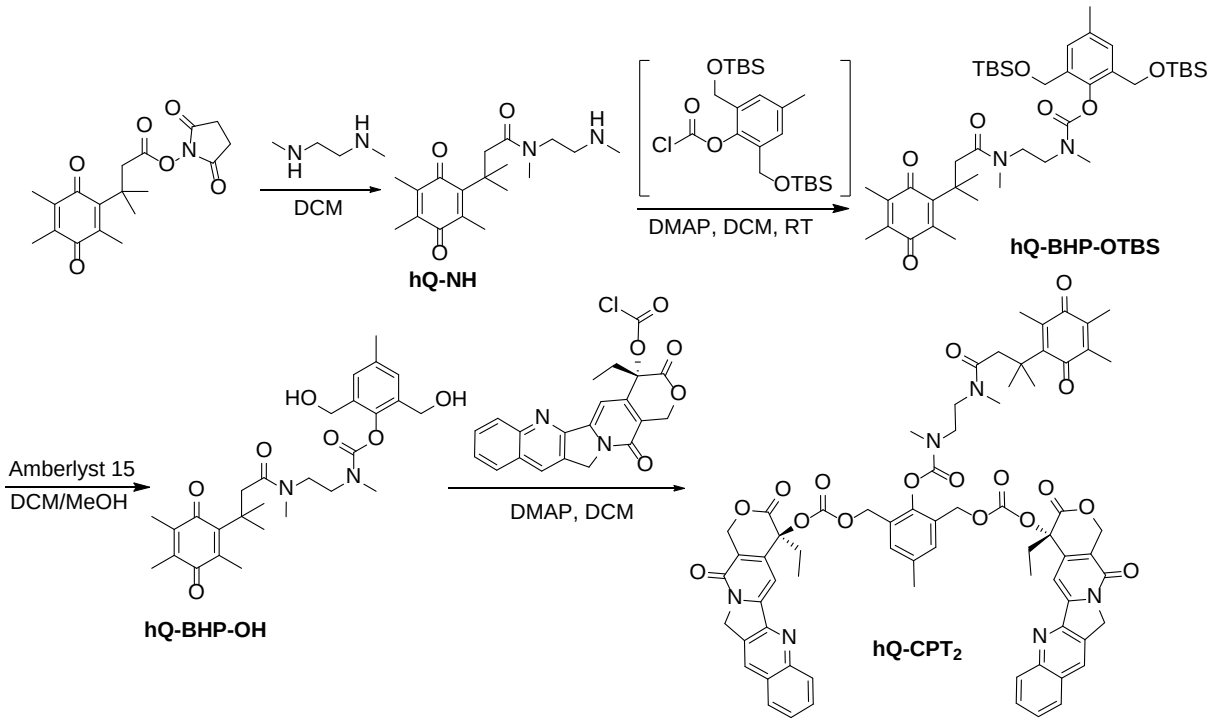

Scheme S1. Synthetic route of hQ-CPT_2.

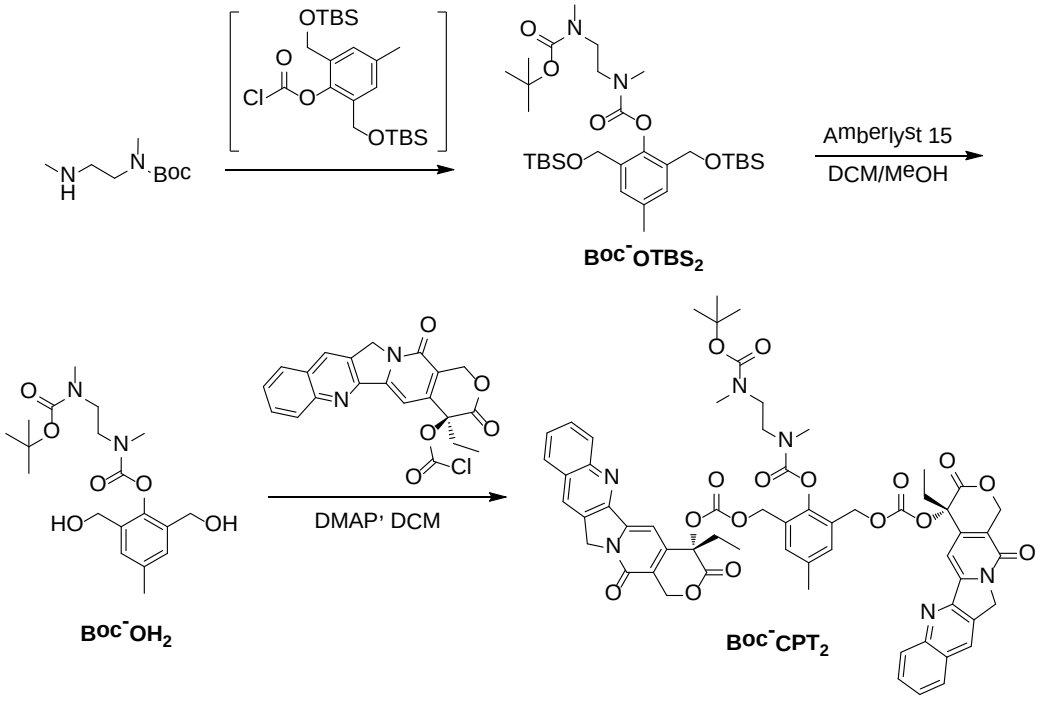

Scheme S2. Synthetic route of Boc-CPT_2.

Table S1. Sequences of primers used for the real-time PCR analysis.

Primer	Sequence
MTA-1 F	5’-ACGCAACCCTGTCAGTCTG-3’
MTA-1 R	5’-GGGCAGGTCCACCATTTCC-3’
GAPDH F	5’-GGTTGTCTCCTGCGACTTCA-3’
GAPDH R	5’-TGGTCCAGGGTTTCTTACTCC-3’

Table S2. Full names and abbreviations of various NPs.

Full name	Abbreviation
hQ-CPT_2-encapsulated nanoparticles	hQC NPs
Boc-CPT_2- and Ce6-co-encapsulated nanoparticles	BocCC NPs
hQ-CPT_2- and Ce6-co-encapsulated nanoparticles	hQCC NPs
hQ-CPT_2- and DiR-co-encapsulated nanoparticles	hQCD NPs

Table S3. Size and drug loading of different NPs.

	Size (nm)	DLE (%)		DLC (%)	
		CPT dimer	Ce6	CPT dimer	Ce6
hQC	93 ± 2	100	—	50	—
hQCC	93 ± 2	100	44.2	46.8	6.5
BocCC	101 ± 2	65.3	18.8	36.5	3.4

Table S4. IC_{50} (μg/mL) of CPT in hQC NPs toward 4T1 and MCF-7 cells under normoxic or hypoxic conditions.

	4T1	MCF-7
Normoxia	82.2	70.5
Hypoxia	8.1	8.5

Table S5. IC_{50} of CPT and Ce6 and CI values between CPT and Ce6 in various NPs toward 4T1 and MCF-7 cells.

	4T1		MCF-7	
	IC_{50} (μg/mL)	CI	IC_{50} (μg/mL)	CI
CPT[a]	82.2	0.44	70.5	0.45
Ce6[b]	2.8		5.2	
CPT[c]	3.3		7.5	
Ce6[c]	0.7		1.8	

[a] hQC NPs; [b] BocCC NPs; [c] hQCC NPs.

Table S6. IC_{50} (μg/mL) of CPT in hQCC NPs toward 4T1 and MCF-7 cells with (w/) or without (w/o) VC pretreatment.

	4T1	MCF-7
w/o VC	3.3	7.5
w/ VC	11.9	17.6

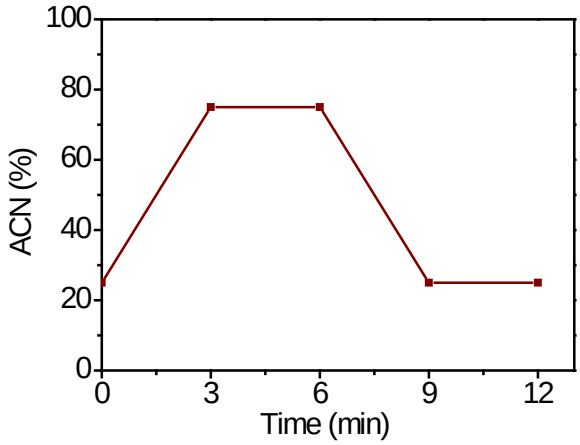

Fig. S1. Time line of the HPLC method as shown by acetonitrile gradient change.

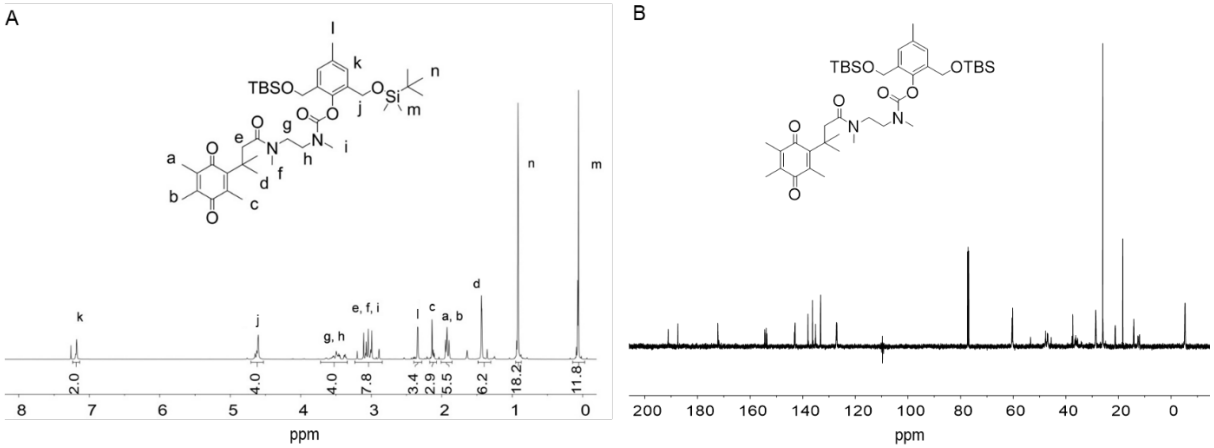

Fig. S2. ^{1}H NMR (A) and ^{13}C NMR (B) spectra of hQ-BHP-OTBS in $CDCl_3$.

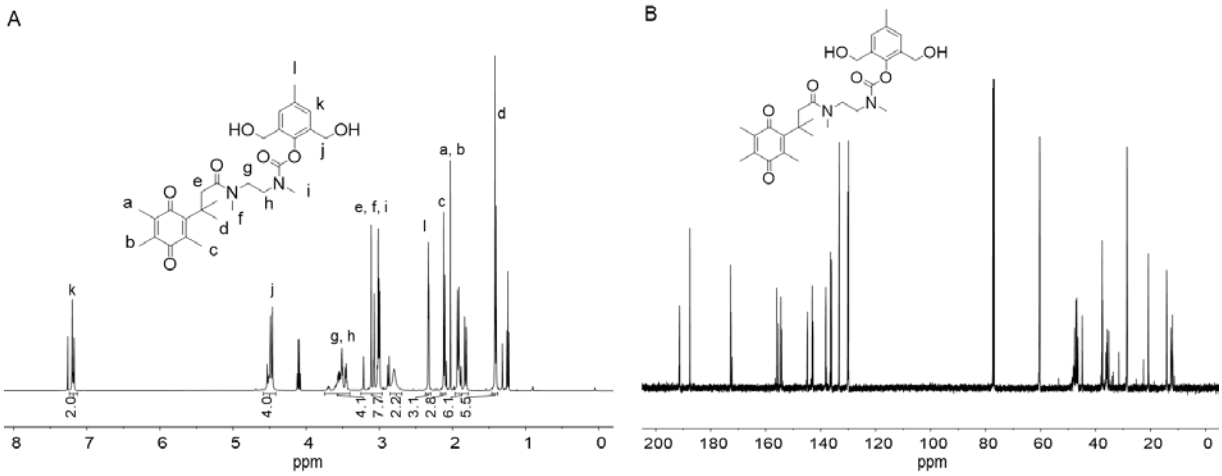

Fig. S3. ^{1}H NMR (A) and ^{13}C NMR (B) spectra of hQ-BHP-OH in $CDCl_3$.

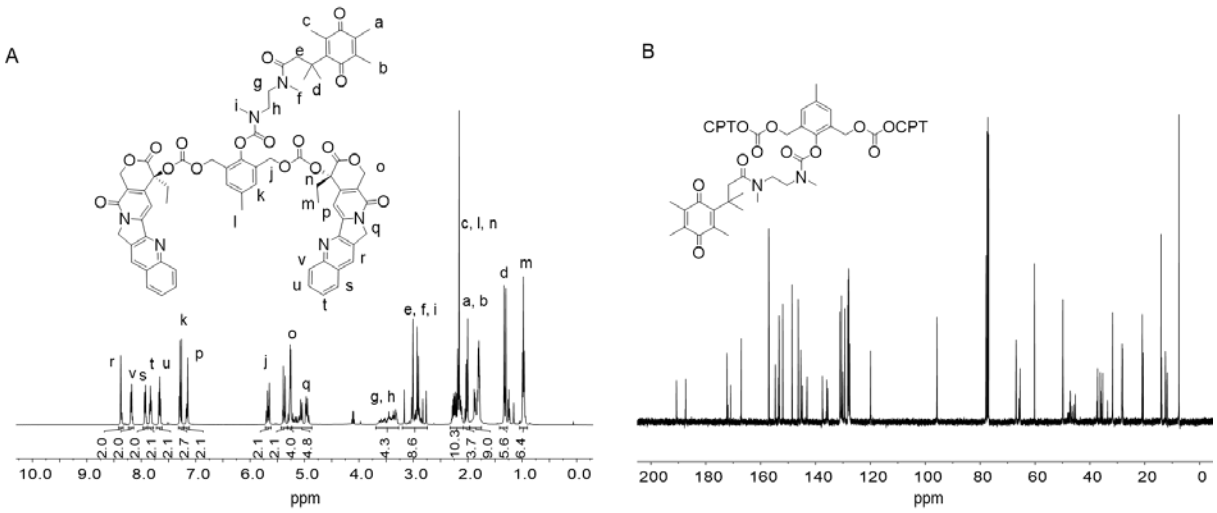

Fig. S4. ^{1}H NMR (A) and ^{13}C NMR (B) spectra of hQ-CPT$_2$ in CDCl$_3$.

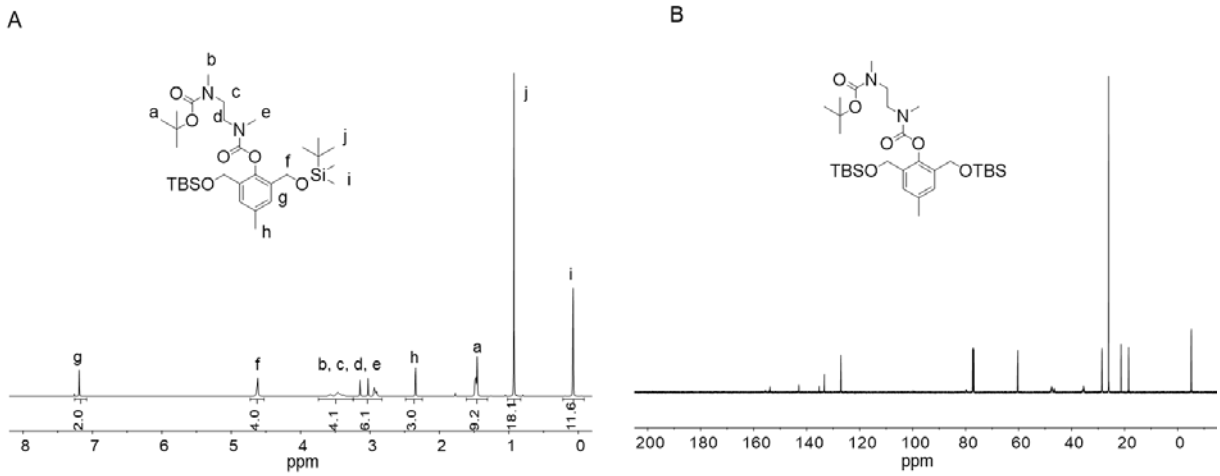

Fig. S5. ^{1}H NMR (A) and ^{13}C NMR (B) NMR spectra of Boc-OTBS$_2$ in CDCl$_3$.

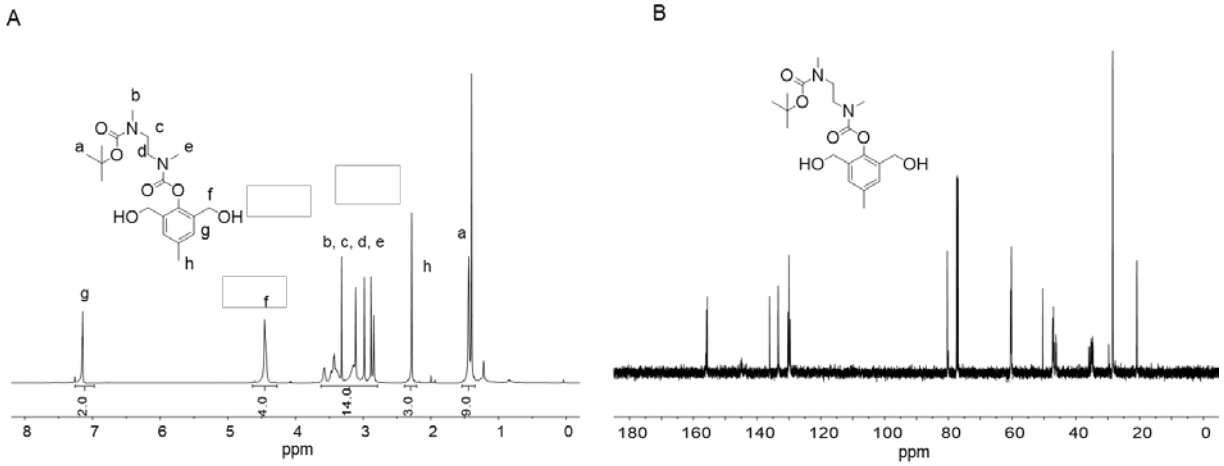

Fig. S6. ^{1}H NMR (A) and ^{13}C NMR (B) spectra of Boc-OH$_2$ in CDCl$_3$.

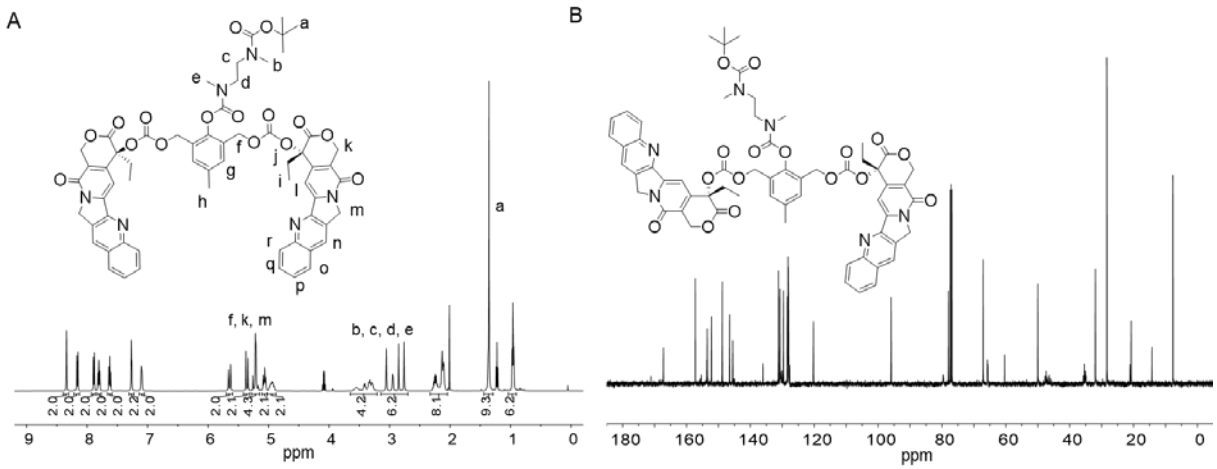

Fig. S7. ^{1}H NMR (A) and ^{13}C NMR (B) spectra of Boc-CPT$_2$ in CDCl$_3$.

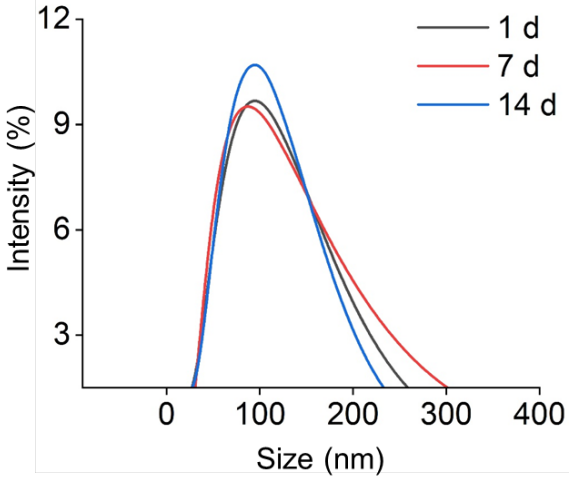

Fig. S8. Size distribution of BocCC NPs after incubation in water at RT for different time.

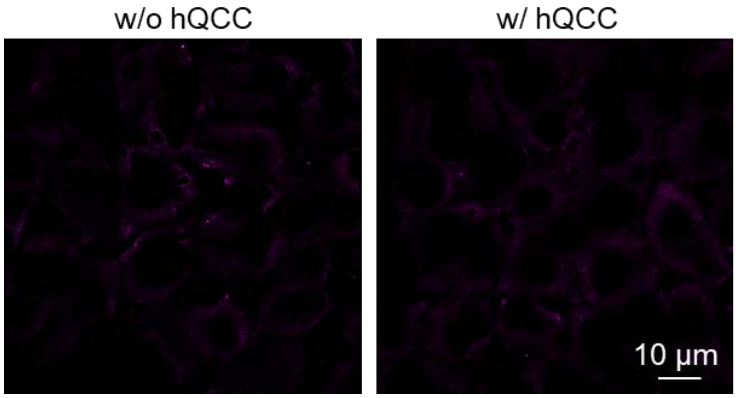

Fig. S9. CLSM images of 4T1 cells with (w/) or without (w/o) 4-h incubation with hQCC NPs (scale bar = 10 μm). The hypoxia level was indicated by the hypoxia/oxidative stress detection mix.

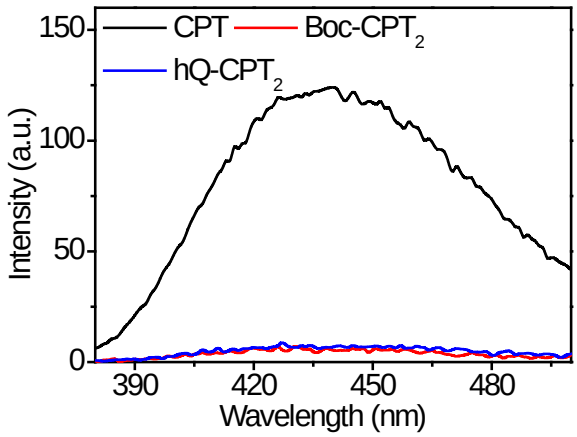

Fig. S10. Fluorescence spectra of CPT, Boc-CPT_2, and hQ-CPT_2 in PBS (1 μg/mL, λ_{ex} = 370 nm).

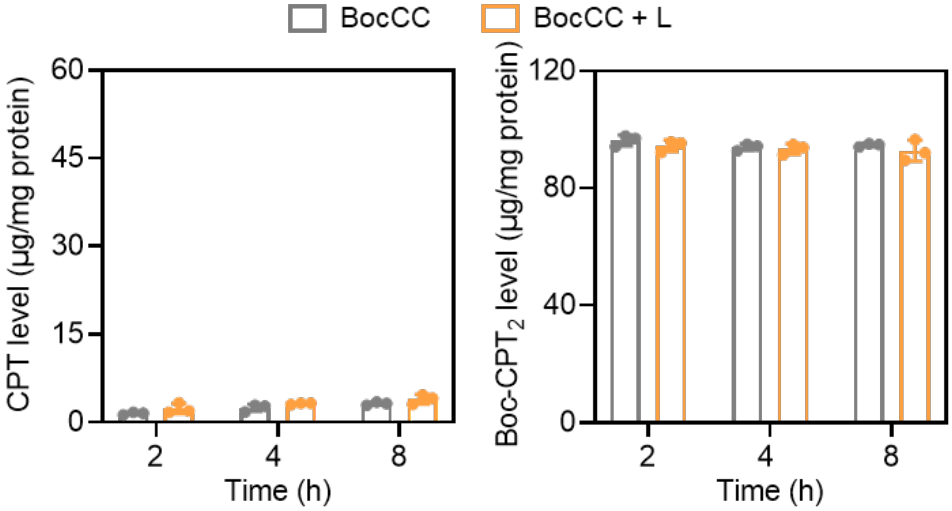

Fig. S11. Contents of CPT and Boc-CPT_2 in 4T1 cells after 24-h incubation with BocCC NPs, 30-min light irradiation (660 nm, 2 mW/cm^2), and further incubation for different time (n = 3).

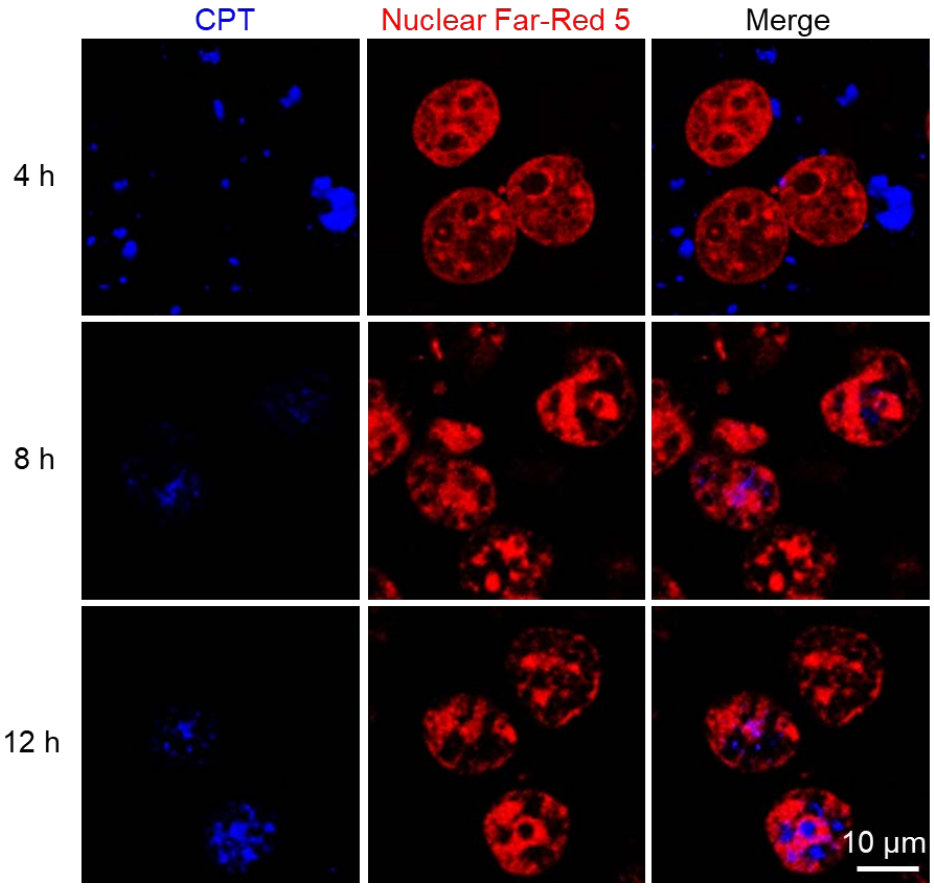

Fig. S12. CLSM images of 4T1 cells after 24-h incubation with hQCC NPs, 30-min light irradiation (660 nm, 2 mW/cm^2), and further incubation for different time (n = 3). Nuclei were stained with Nuclear Far-Red 5.

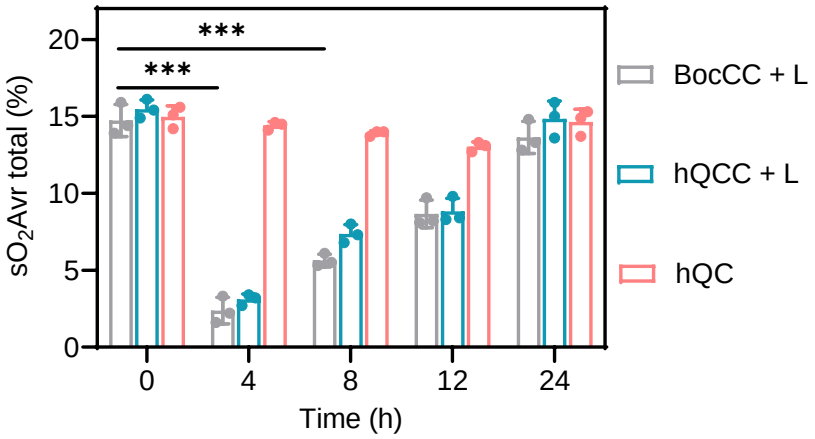

Fig. S13. Quantified oxyhemoglobin saturation levels in the tumors in Fig. 2F (n = 3).

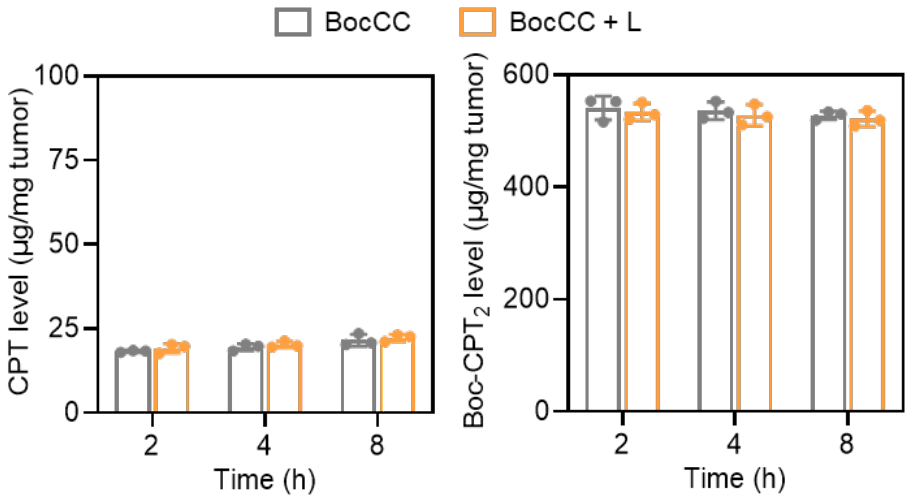

Fig. S14. Contents of CPT and Boc-CPT_2 in 4T1 orthotopic tumors (n = 3). Boc-CPT_2 NPs were intratumorally injected, and tumors were irradiated (660 nm, 10 mW/cm^2, 30 min) at 2, 4, and 8 h post injection.

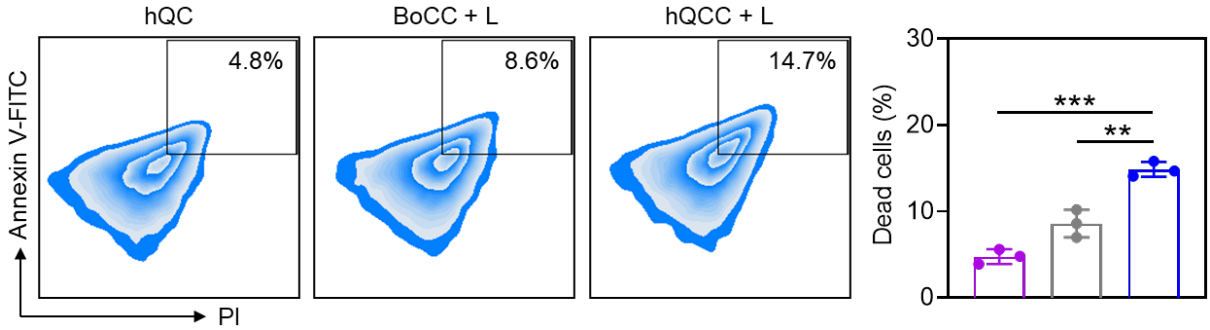

Fig. S15. Flow cytometric histograms of 4T1 cells and the calculated percentages of dead cells (Annexin V^+PI^+) (n = 3). Cells were treated with NPs for 24 h, with or without subsequent light irradiation (660 nm, 2 mW/cm^2, 30 min).

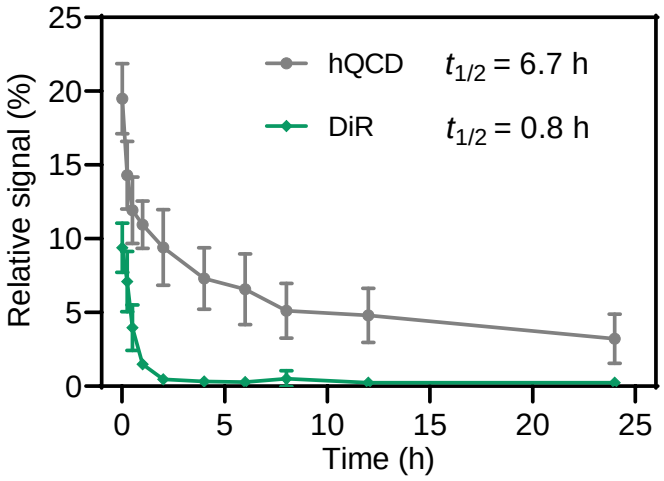

Fig. S16. Pharmacokinetics of hQCD NPs and DiR following *i.v.* injection (n = 3).

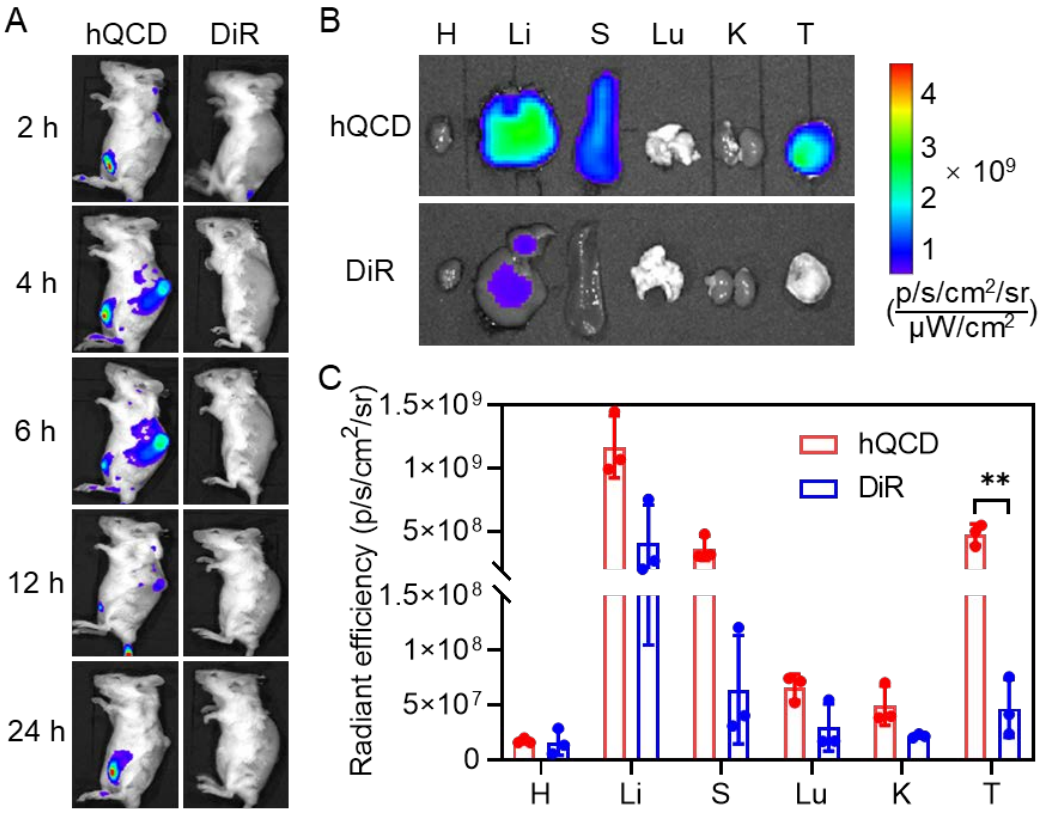

Fig. S17. *In vivo* biodistribution of *i.v.* injected hQCD NPs and DiR (1.25 mg DiR/kg) in 4T1 mammary tumor-bearing mice. (A) *In vivo* fluorescence imaging of mice at 2, 4, 6, 12, and 24 h post injection. (B) *Ex vivo* fluorescence imaging of excised tumors and major organs at 6 h post injection (H: heart; Li: liver; S: spleen; Lu: lung; K: kidney; T: tumor). (C) Calculated fluorescence intensity from *ex vivo* fluorescence imaging in (B) (n = 3).

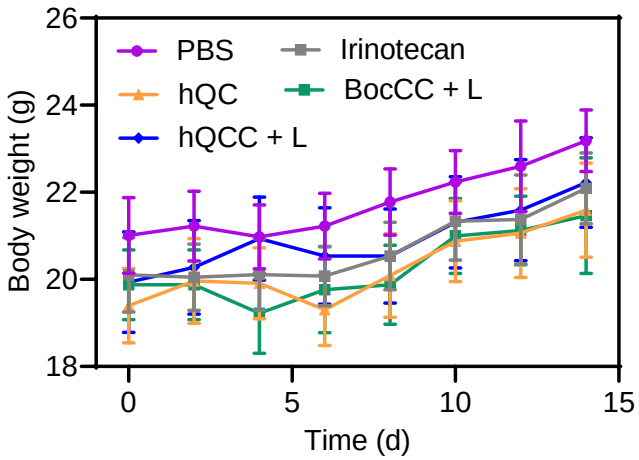

Fig. S18. Body weight changes of 4T1 tumor-bearing mice within the observation period of 14 d (n = 8).

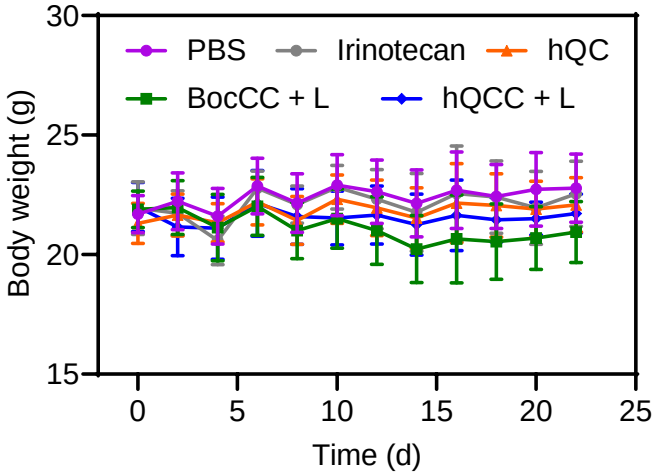

Fig. S19. Body weight changes of MCF-7 tumor-bearing mice within the observation period of 22 d (n = 8).

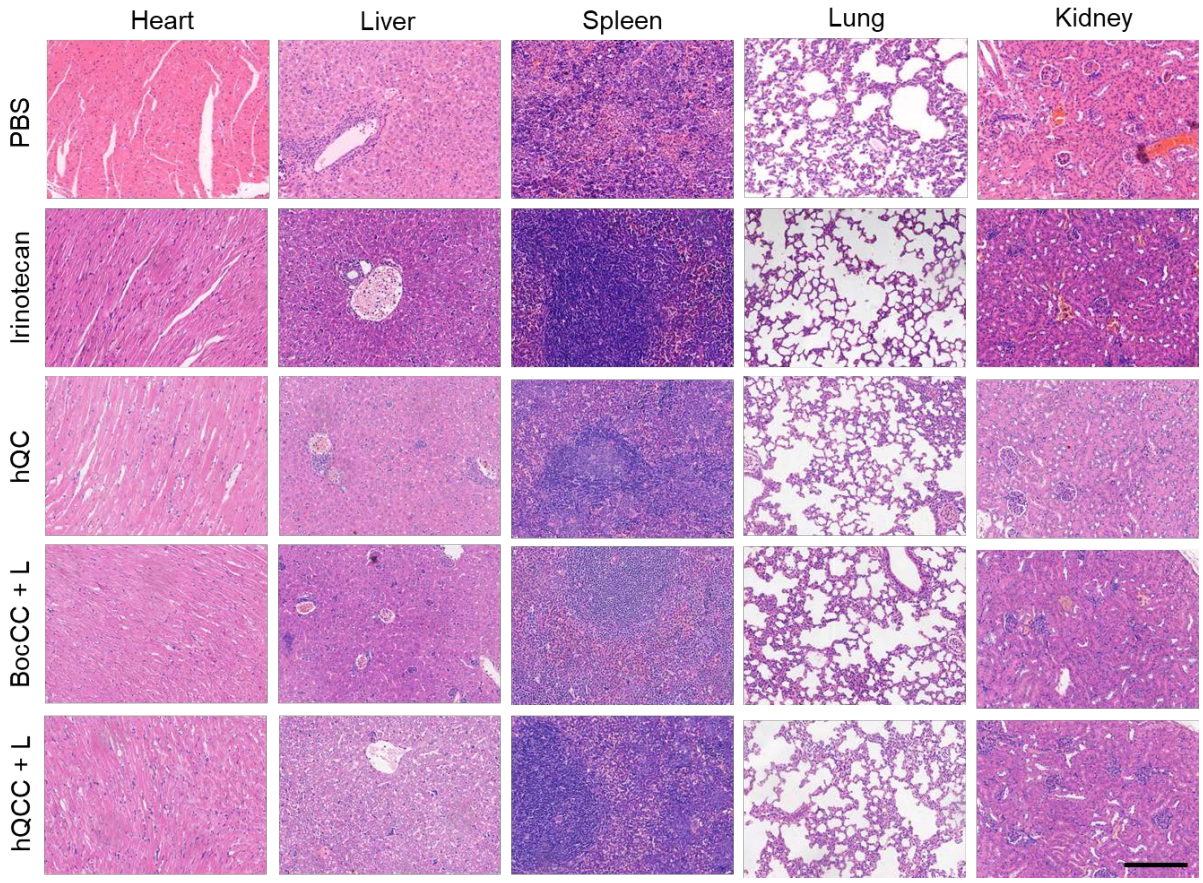

Fig. S20. Representative photomicrographs of H&E-stained major organ sections harvested from 4T1 tumor-bearing mice on day 14 (scale bar = 100 μm).

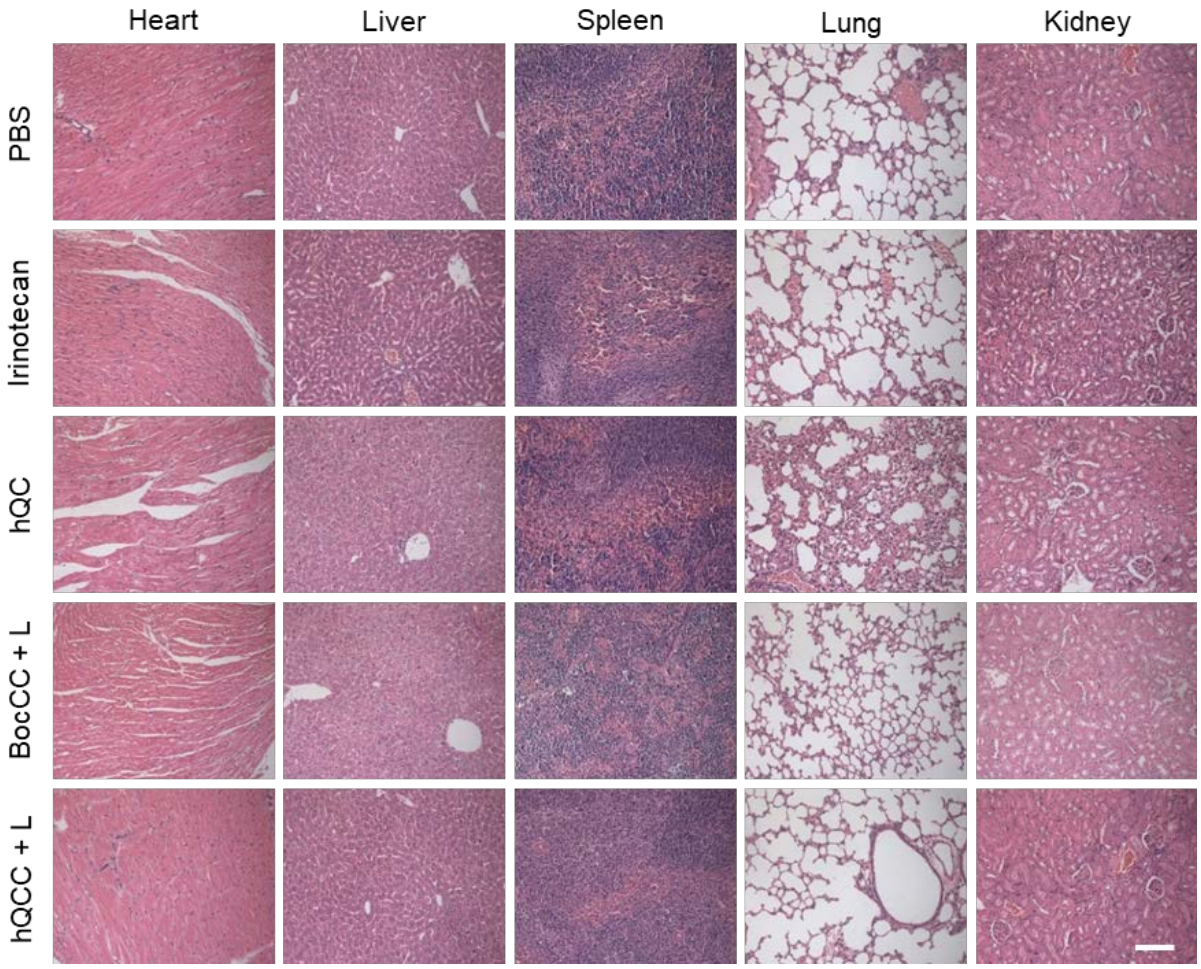

Fig. S21. Representative photomicrographs of H&E-stained major organ sections harvested from MCF-7 tumor-bearing mice on day 22 (scale bar = 100 μm).

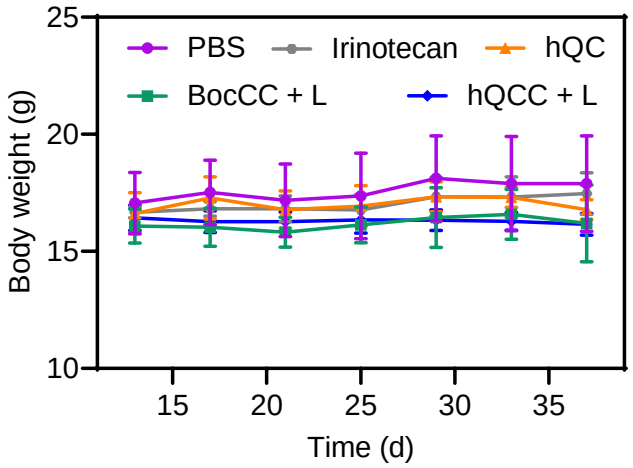

Fig. S22. Body weight change of GFP/Luc-4T1 tumor-bearing mice within the observation period of 40 d (n = 6).

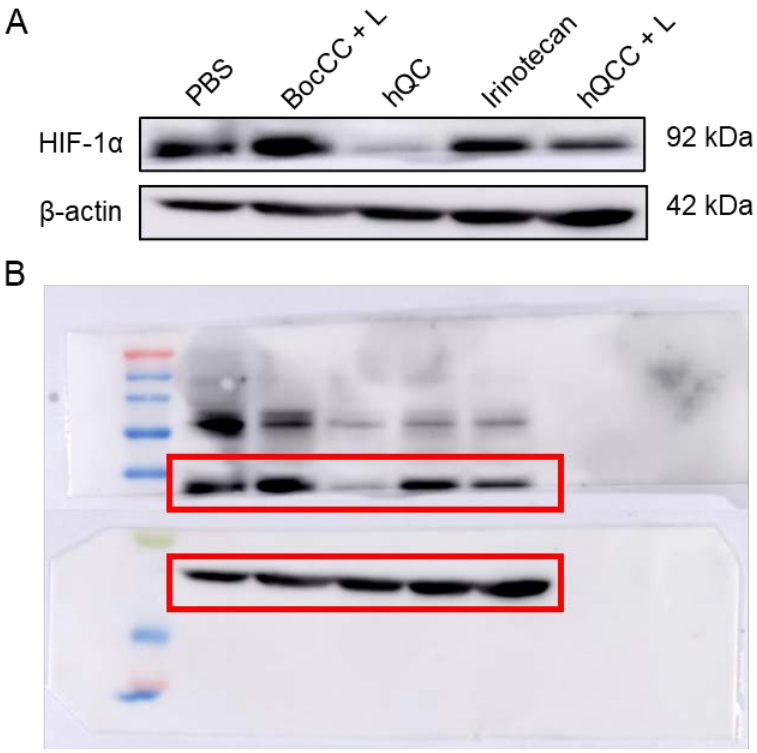

Fig. S23. (A) HIF-1α levels in tumors harvested from GFP/Luc-4T1 tumor-bearing mice at 18 h post light irradiation as resolved by Western blot. (B) Uncropped Western blots. Cropping is designated by the red boxes.